Fibers and Polymers 2019, Vol.20, No.12, 2665-2671
DOI 10.1007/s12221-019-9636-y

ISSN 1229-9197 (print version)
ISSN 1875-0052 (electronic version)

Note

Injection Molding of Carbon Fiber Composite Automotive Wheel

Zheng Min Huang[1], Hyung Min Kim[1], Jae Ryoun Youn[1]*, and Young Seok Song[2]*

[1]*Research Institute of Advanced Materials (RIAM), Department of Materials Science and Engineering, Seoul National University, Seoul 08826, Korea*
[2]*Department of Fiber System Engineering, Dankook University, Yongin 16890, Korea*

(Received June 16, 2019; Accepted June 26, 2019)

Abstract: Injection molding (IM) is a manufacturing process that produces polymeric parts by injecting molten thermoplastic polymer into a mold cavity. It mainly fabricates geometrically complicated parts with dimensional accuracy. In this paper, injection molding of carbon fiber composite automotive wheels with complex shape was investigated numerically. Insert injection molding was also considered to reduce the deformation of the part. Injection molding conditions were determined based on the simulation results such as filling time, mechanical property, and warpage for manufacturing of composite automotive wheels.

Keywords: Injection molding, Numerical simulation, Carbon fiber composite, Automotive wheel

Introduction

Improving fuel efficiency becomes an important issue in the automotive industry. For this, hybrid engines and lightweight components are applied to automobiles. Among them, reducing weight of the wheel by employing the composite rim is one of challenging issues. In recent years, the wheels have been manufactured using fiber reinforced composites, but it is still not feasible to produce them by injection molding [1,2].

Injection molding is a cost and time efficient processing method for mass production of polymeric parts. It is also environmentally friendly compared with other methods since it uses thermoplastic polymer in a closed environment. It has recently been used to produce parts with complex shapes and small dimensions such as micro- and nano-scales [3-5]. Injection molding process can be modeled numerically to understand the entire steps such as filling, packing, cooling, and ejection stages [6-20]. Numerical simulation will save cost and time in designing and manufacturing polymeric parts by optimizing processing conditions.

In this study, numerical analysis was carried out to manufacture a thick and complex automotive wheel with carbon fiber composite. The resin flow during filling and deformation of parts at ejection were predicted numerically. Insert injection molding was also considered to reduce the deformation of the part and improve the mechanical properties. The insert injection molded part was assessed in terms of pressure, fiber orientation, deformation, elastic modulus, and residual stress distribution.

*Corresponding author: jaeryoun@snu.ac.kr
*Corresponding author: ysong@dankook.ac.kr

Experimental

A finite element method (FEM) simulation program, Moldex3D®, was used in this study. The entire processing steps, filling, packing, cooling, and warpage stages, were modeled for injection molding of carbon fiber composite automotive wheels. The resin flow in the mold is governed by the following equations [21].

$$\frac{d\rho}{dt} + \rho(\nabla \cdot \tilde{v}) = 0 \tag{1}$$

$$\rho\frac{d\tilde{v}}{dt} = -\nabla P + \nabla \cdot \tilde{\tau} + \rho\tilde{g} \tag{2}$$

$$\rho C_p\frac{dT}{dt} = \beta T\frac{dP}{dt} + \eta\dot{\gamma} + \nabla \cdot \tilde{q} \tag{3}$$

where ρ is the density, $\tilde{v}$ is the velocity vector, P is the pressure, $\tilde{\tau}$ is the stress tensor, $\tilde{g}$ is the gravity vector, C_p is the specific heat at constant pressure, β is the thermal expansion coefficient, η is the generalized Newtonian viscosity, $\tilde{q}$ is the heat flux vector, and $\dot{\gamma}$ is the magnitude of shear rate tensor.

Figure 1(a) shows the shape of the automotive wheel. Geometric modeling and finite element generation were carried out (Figure 1(b)-(d)). More than 2 million finite elements were generated by employing tetrahedral, prism, pyramid, and hexagonal elements. The diaphragm gate was selected (Figure 2(a)) and the size and shape of the sprue, gate, and runner were determined. As shown in Figure 2(b), the conformal cooling channel was considered and the nine cooling lines have the spiral structure. The entire mold has a size of 1200 mm×1200 mm×1200 mm (Figure 2(c)). For numerical simulation, two cases were taken into account: Case 1 without insert and Case 2 with metallic insert (Figure

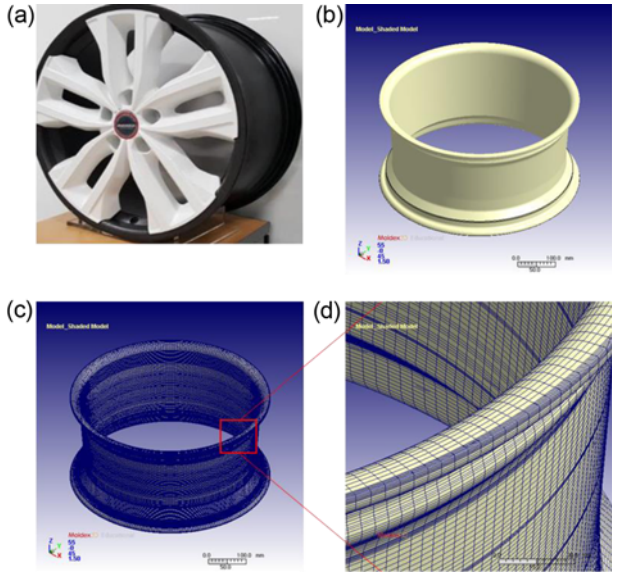

Figure 1. (a) Automotive wheel considered in this study, (b) CAD model, (c) finite element mesh, and (d) magnified mesh structure.

3). The insert parts were positioned at upper and lower locations in the automotive wheel as shown in Figure 3(b). 40 wt% carbon fiber filled Polyamide 6 (PA6) (Akro-plastic Corporation (AKROMID B3 ICF 40)) and aluminum insert were taken into account for the simulation. The material properties for numerical analysis were obtained from Moldex3D. Processing conditions are listed in Table 1.

Table 1. Process conditions used in the simulation

	w/o insert	w/ insert
Filling time	7 s	1.5 s
Packing time	70 s	55 s
Cooling time	900 s	
Melt temperature	285 °C	
Initial insert part temperature	-	80 °C
Mold temperature	80 °C	
Freeze temperature	186 °C	
Ejection temperature	166 °C	

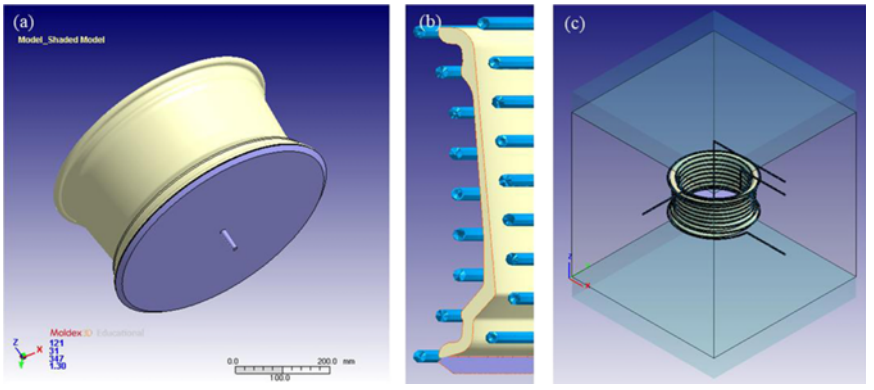

Figure 2. Geometry of (a) runner and gate, (b) cooling channel, and (c) mold.

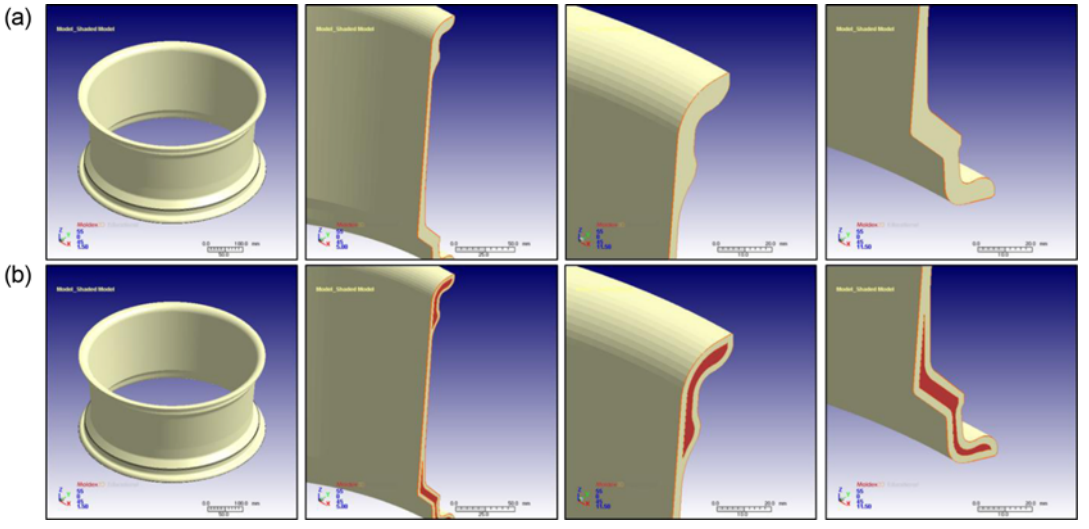

Figure 3. Geometry of (a) Case 1 without insert and (b) Case 2 with insert.

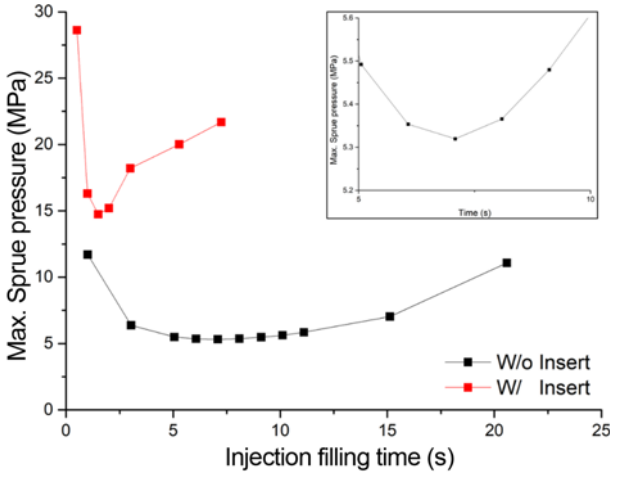

Figure 4. Sprue pressure w.r.t. the filling time.

Results and Discussion

The sprue pressure required to fill the cavity is shown as a function of the filling time in Figure 4. High melt velocity needs high injection pressure to fill the mold cavity and high sprue pressure is required to achieve short filling time. The sprue pressure showed a minimum value in the graph for the cases without and with insert with respect to the filling time, which allowed us to determine the optimum filling times (i.e., 7 s without insert and 1.5 s with insert). The freezing time at the gate was also predicted by the simulation. The packing time without and with insert was 70 s and 55 s, respectively (Figure 5). The initial temperature of the aluminum insert was set at 80 °C. Since minimum cooling time typically indicates the time when 80 % of cavity and 60 % of runner are solidified, the cooling time was increased to 900 s.

Figure 6 shows the melt front advancement in the cavity with respect to time. The resin filled the circular runner first and infused into the cavity. The filling time was 7.077 s for Case 1 and 1.514 s for Case 2. Higher pressure was required for Case 2 because its filling time was shorter than that of Case 1. Therefore, Case 2 showed higher pressure field than Case 1 as shown in Figure 7(a,b). Total weight of Case 2 was higher than that of Case 1 (Figure 7(c)) because the density of aluminum (i.e., 2.7×10^3 kg/m^3) is higher than that of polymer (i.e., 1.31×10^3 kg/m^3).

The fiber orientation was predicted as shown in Figure 8. Since the resin mainly flowed in the vertical direction, fibers were oriented along that direction in both cases (Figure 8). It was found that the two cases had quite similar fiber orientation.

Figure 9 presents the elastic modulus of the molded part in x, y and z directions. The average modulus in each direction is given in the figure. Case 2 with insert showed higher values in every direction because of the aluminum insert.

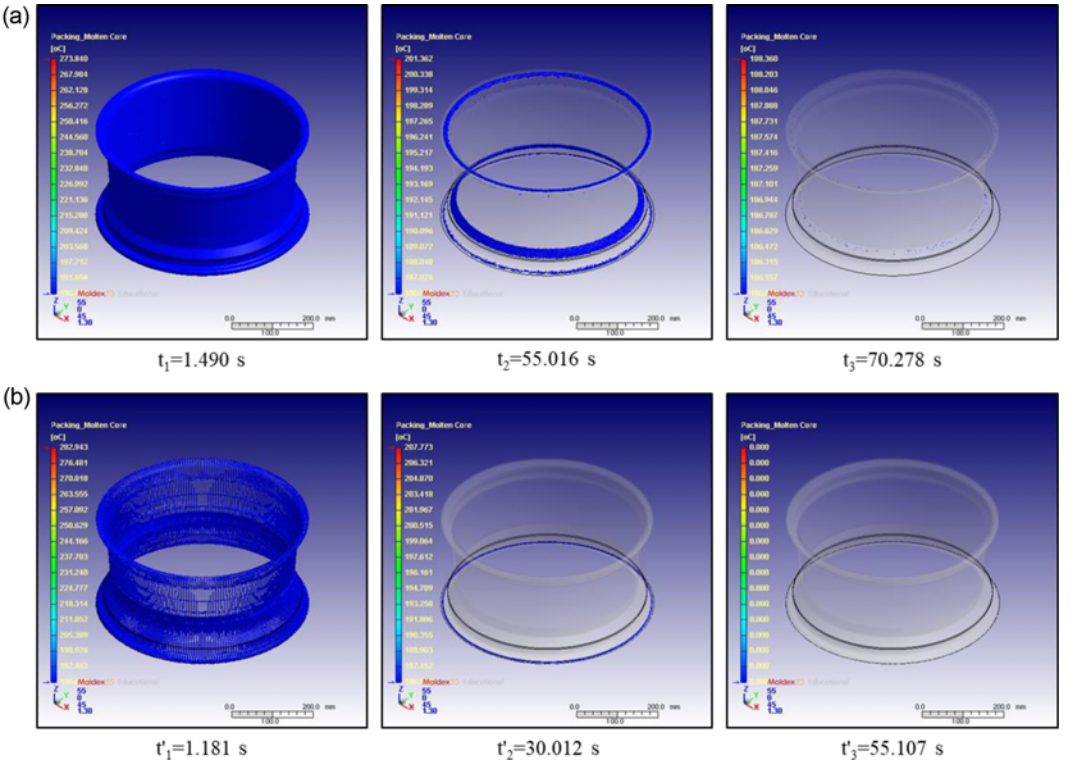

Figure 5. Existing polymer melt w.r.t. time; (a) Case 1 and (b) Case 2.

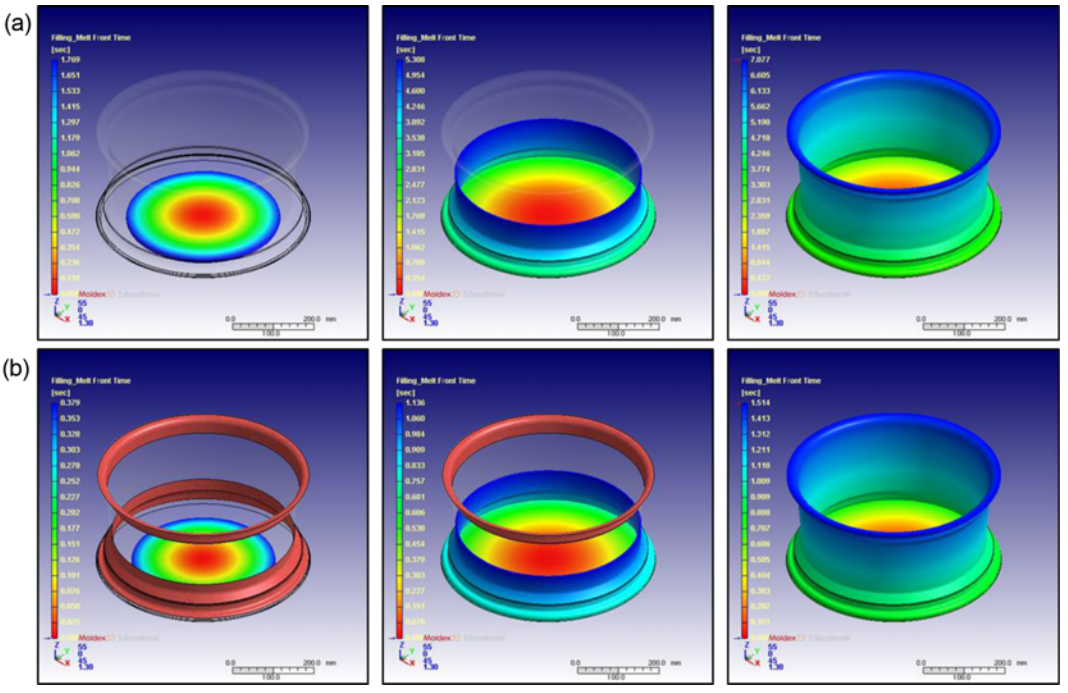

Figure 6. Melt front advancement in the cavity w.r.t. time; (a) Case 1 and (b) Case 2 at 25 %, 75 %, and 100 % filling.

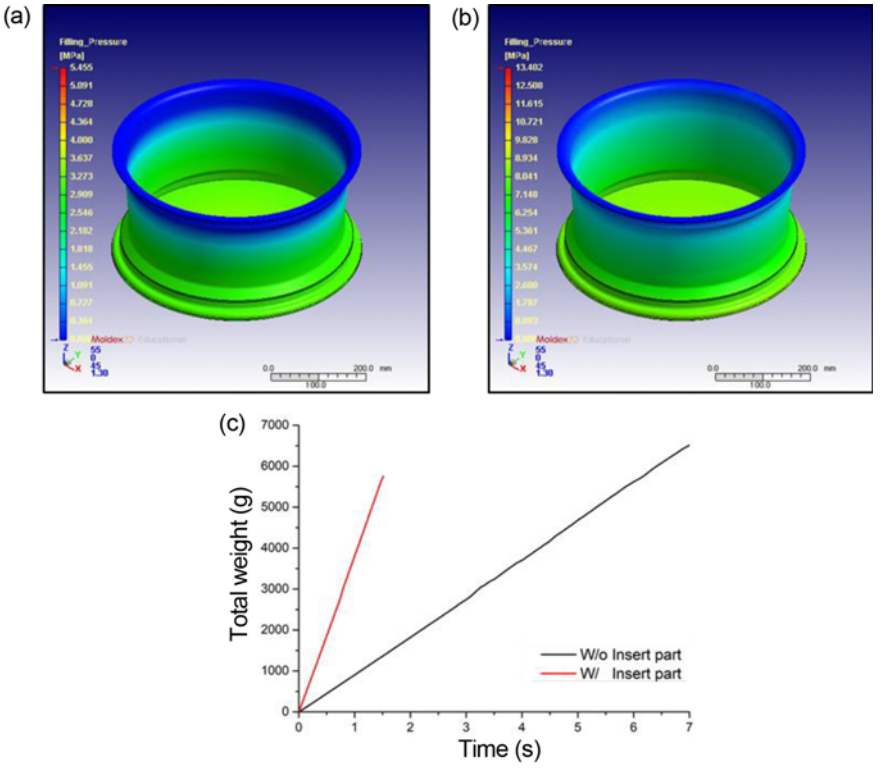

Figure 7. Pressure distribution after 100 % filling; (a) Case 1, (b) Case 2, and (c) comparison of the total weight between the two cases.

The elastic modulus of aluminum is 68 GPa, and that of the carbon fiber is 38.2 GPa in the longitudinal direction and 10.3 GPa in the transverse direction. For both cases, the modulus in the z direction is higher than that in the x and y directions due to the fiber orientation.

The total deformation and thermal residual stress of the

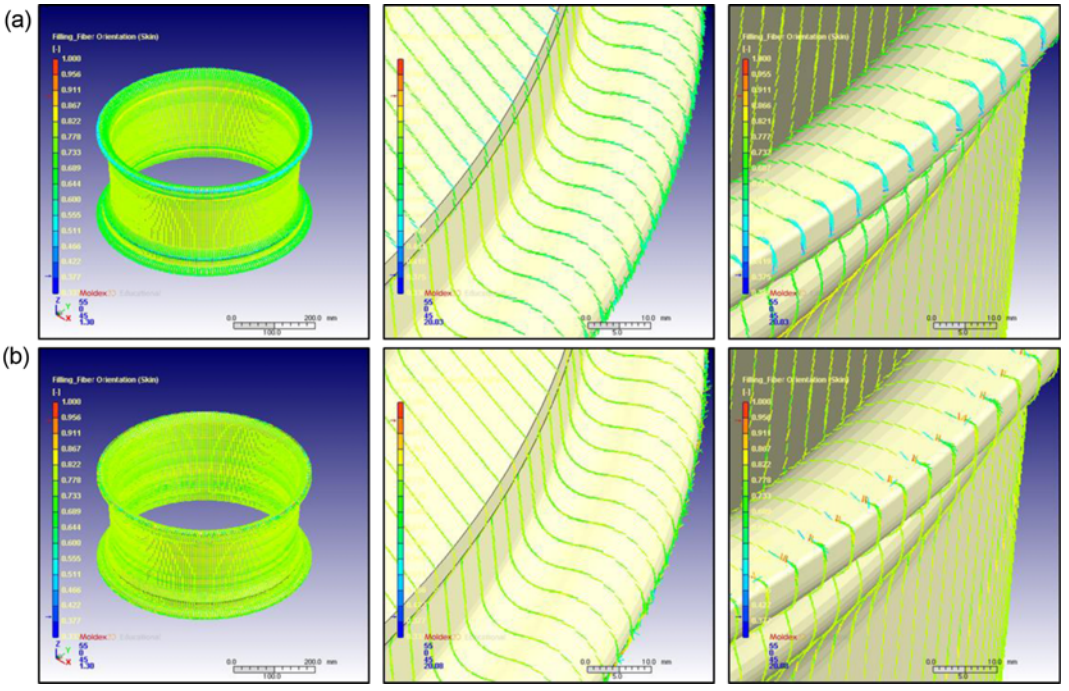

Figure 8. Fiber orientation at the skin layer; (a) Case 1 and (b) Case 2.

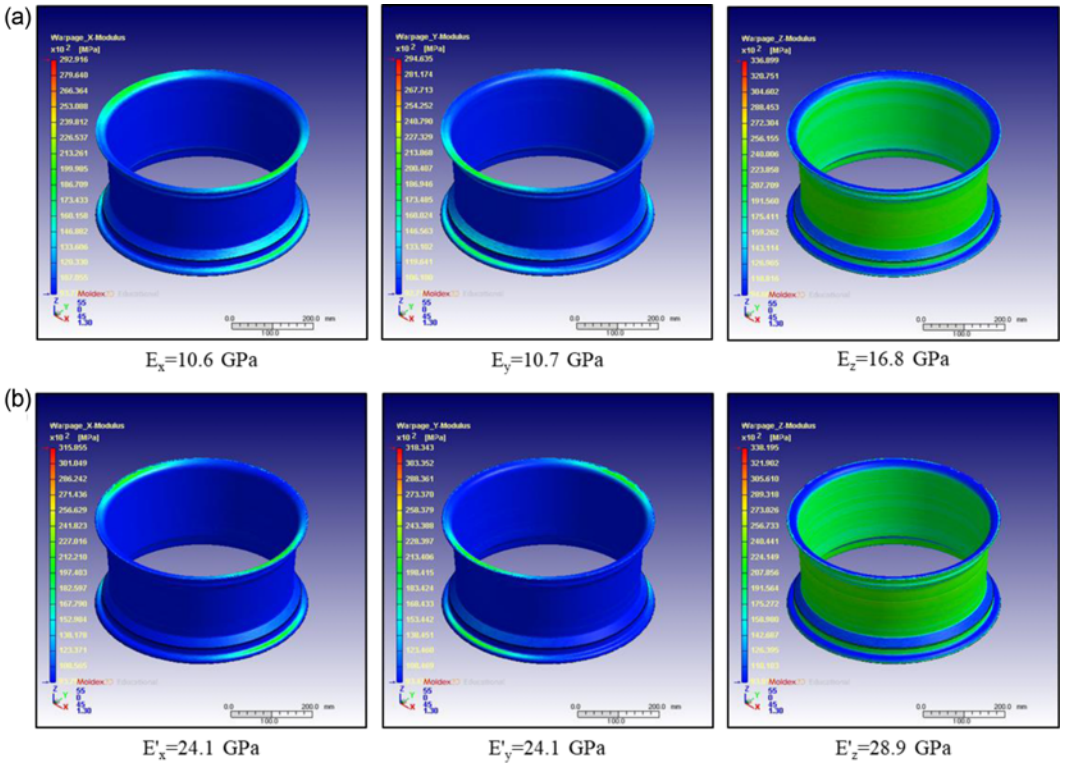

Figure 9. Elastic modulus of the molded part in the x, y and z direction; (a) Case 1 and (b) Case 2.

molded part are shown in Figure 10. For Case 1, the deformation increased as the distance from the gate became larger (Figure 10(a)). It was found in Case 2 that the deformation was significantly reduced at the upper and lower locations where the insert part was located (Figure 10(b)). However, the deformation in the middle was

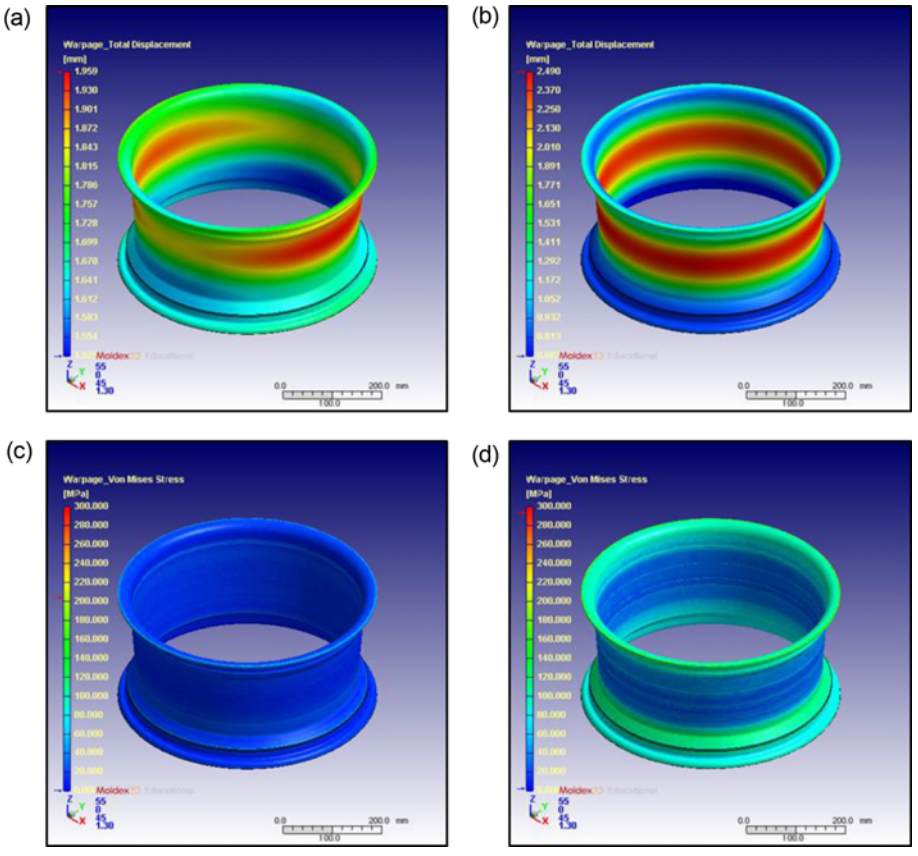

Figure 10. Total deformation and thermal residual stress of the molded part for Case 1 ((a) and (c)) and Case 2 ((b) and (d)).

increased to 2.5 mm. On the other hand, the residual stress of Case 2 was higher than that of Case 1, especially in the middle region. Consequently, the molded rim with insert achieved significant improvement in the deformation.

Conclusion

3D numerical simulation of injection molding was carried out for automotive wheel. The resin flow and warpage of the product were investigated numerically. The filling time in the cavity was optimized and the gate freezing time was determined. The effect of insert on the injection molded part was also evaluated. It was found that the deformation of the part was reduced significantly when the insert was applied. This study will provide a meaningful guideline for manufacturing of a real automotive wheel via injection molding.

References

1. J.-H. Hong, S.-H. Yoo, and S.-H. Chang, *Compos. Res.*, **26**, 386 (2013).
2. W. Xiaoyin, L. Xiandong, S. Yingchun, W. Xiaofei, L. Wanghao, and P. Yue, *P. I. Mech. Eng. C-J. Mec.*, **230**, 1634 (2016).
3. V. Bellantone, R. Surace, G. Trotta, and I. Fassi, *Int. J. Adv. Manuf. Tech.*, **67**, 1407 (2013).
4. G. Lucchetta, M. Sorgato, S. Carmignato, and E. Savio, *CIRP Ann.*, **63**, 521 (2014).
5. H. J. Oh and Y. S. Song, *RSC Adv.*, **5**, 99797 (2015).
6. S. Kitayama, M. Yokoyama, M. Takano, and S. Aiba, *Int. J. Adv. Manuf. Tech.*, **92**, 3991 (2017).
7. S. A. Jahan, T. Wu, Y. Zhang, J. Zhang, A. Tovar, and H. Elmounayri, *Procedia Manuf.*, **10**, 898 (2017).
8. S. Laurenzi, A. Grilli, M. Pinna, F. De Nicola, G. Cattaneo, and M. Marchetti, *Compos. Part B-Eng.*, **57**, 47 (2014).
9. X. Li, N. Gong, Z. Gao, and C. Yang, *Int. J. Adv. Manuf. Tech.*, **90**, 1457 (2017).
10. B. Kim and J. Min, *J. Mater. Process. Tech.*, **245**, 215 (2017).
11. H. Zhou, "Computer Modeling for Injection Molding: Simulation, Optimization, and Control", John Wiley & Sons, Hoboken, 2013.
12. Y. Wang, K.-M. Yu, and C. C. Wang, *Comput. Aided Des.*, **63**, 1 (2015).
13. M. Azaman, S. Sapuan, S. Sulaiman, E. Zainudin, and A. Khalina, *Mater. Des. (1980-2015)*, **52**, 1018 (2013).
14. F. Hsu, K. Wang, C. Huang, and R. Chang, *Adv. Prod. Eng. Manage.*, **8**, 107 (2013).

15. O. A. Mohamed, S. Masood, and A. Saifullah, *Int. J. Eng. Res.*, **2**, 344 (2013).
16. Y. Xu, Q. Zhang, W. Zhang, and P. Zhang, *Int. J. Adv. Manuf. Tech.*, **76**, 2199 (2015).
17. R. Spina, M. Spekowius, R. Dahlmann, and C. Hopmann, *Int. J. Precis. Eng. Man.*, **15**, 89 (2014).
18. E. Oliaei, B. S. Heidari, S. M. Davachi, M. Bahrami, S. Davoodi, I. Hejazi, and J. Seyfi, *J. Mater. Sci. Technol.*, **32**, 710 (2016).
19. M. Azaman, S. Sapuan, S. Sulaiman, E. Zainudin, and A. Khalina, *Polym. Eng. Sci.*, **55**, 1082 (2015).
20. M. Khan, S. K. Afaq, N. U. Khan, and S. Ahmad, *ISRN Mech. Eng.*, **2014**, 8 (2014).
21. Y. I. Kwon and Y. S. Song, *Korea-Aust. Rheol. J.*, **30**, 161 (2018).